Translational profiling of mouse dopaminoceptive neurons reveals region-specific gene expression, exon usage, and striatal PGE2 modulatory effects

Enrica Montalban et al.

SUPPLEMENTARY FIGURES

List of Figures:

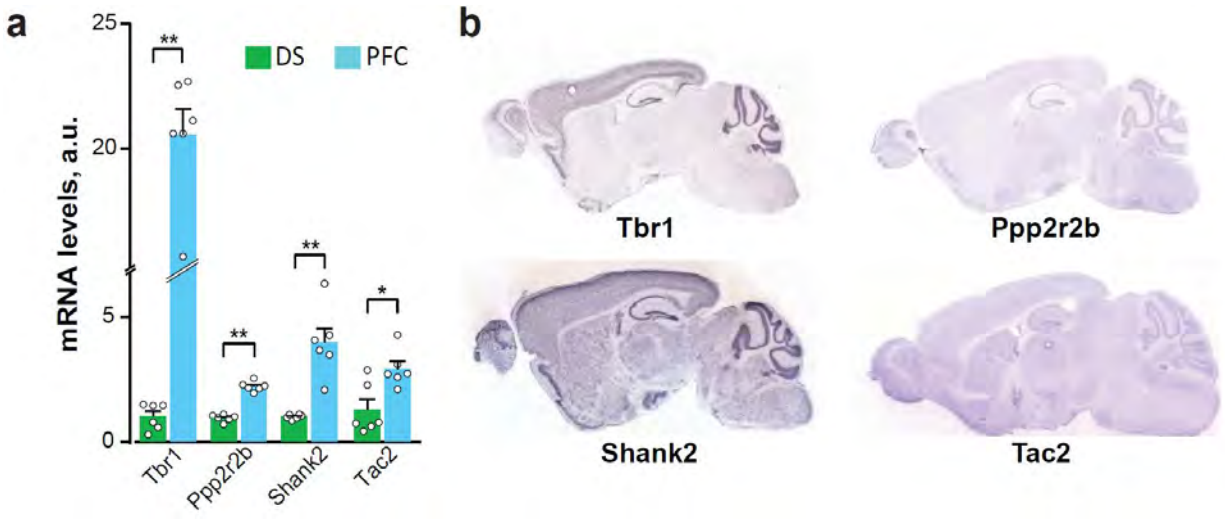

Supplementary Figure 1: Confirmation of TRAP-Seq mRNA differences between PFC and striatum by RT-qPCR and *in situ* hybridization for selected genes.

a. Genes with diverse levels of differential expression in RNA seq in the regional BAC-TRAP analysis were selected for RT-qPCR verification using wild-type mouse brain. The expression levels were calculated by the comparative ddCt method with *Ppia* as an internal control. Data points are individual results from different mice (n = 4-6 per group). Means + SEM are indicated. Statistical analyses with two-tailed Mann-Whitney's test, *p < 0.05; **p < 0.01. Detailed statistical results in **Supplementary Table 19**. **b.** *In situ* hybridization patterns from the Allen Brain Institute (http://mouse.brain-map.org/) for the genes studied by RT-qPCR in (**a**). For gene products with strong enrichment and high expression levels the hybridization differences are easily visible (e.g. *Tbr1* in cortex), whereas for other gene products, RNA-Seq and RT-qPCR are more informative (e.g. *Ppp2r2b*, *Shank2*, *Tac2*).

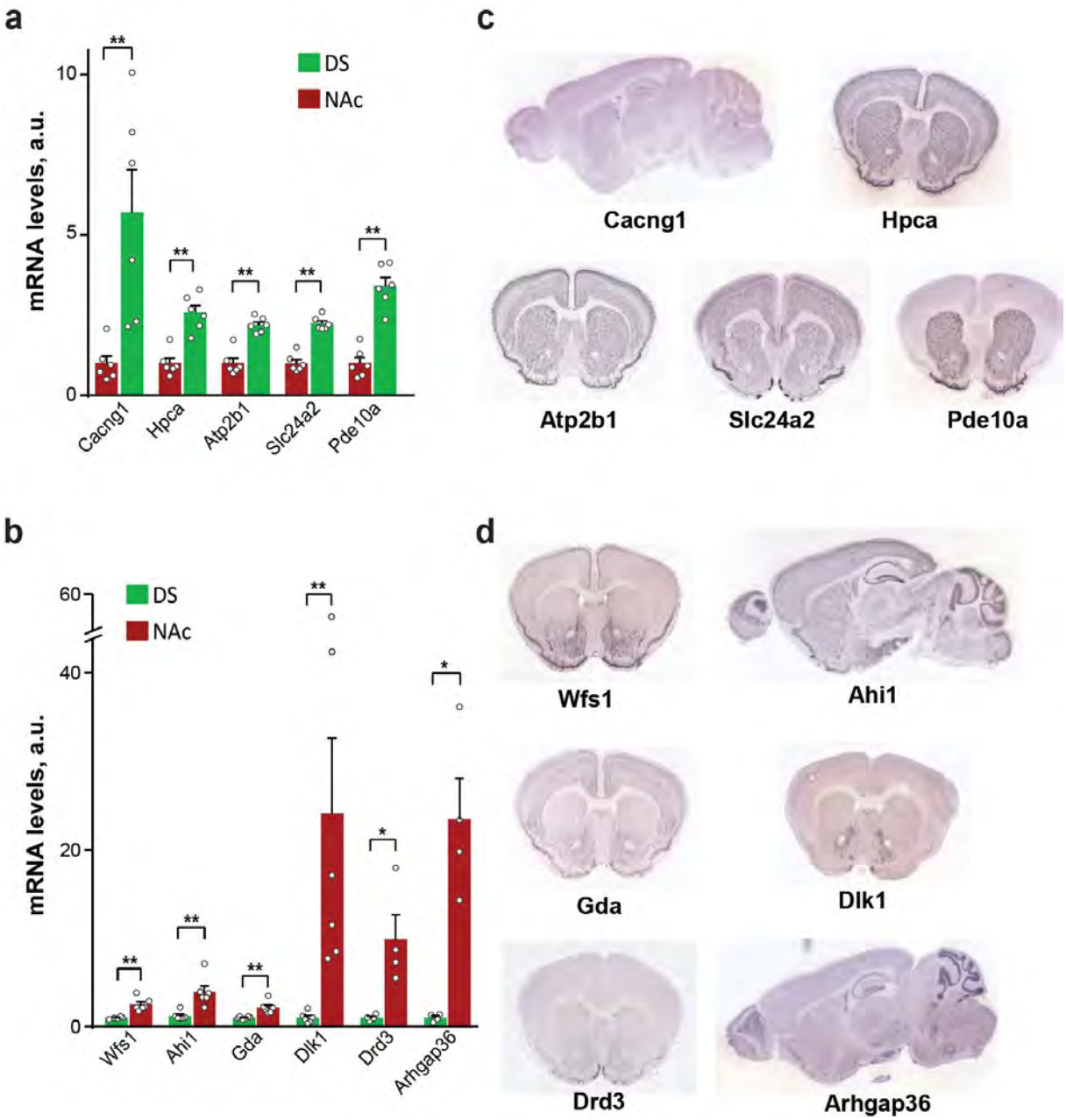

Supplementary Figure 2: Confirmation of TRAP-Seq mRNA differences between DA and NAc by RT-qPCR and *in situ* hybridization for selected genes.

a-b. Genes more expressed DS than in the NAc (**a**) or in the NAc than in the DS (**b**), with diverse levels of differential expression in the TRAP-Seq regional analysis were selected for quantitative PCR verification using wild-type mouse brain. Expression levels were calculated by the comparative ddCt method with *Myh7* as an internal control. Data points are individual results from different mice (n = 4-6 per group). Means + SEM are indicated. Statistical analyses with two-tailed Mann-Whitney's test, *p < 0.05; **p < 0.01. Detailed statistical results in **Supplementary Table 19**. **c-d.** *In situ* hybridization patterns from the Allen Brain Institute (http://mouse.brain-map.org/) for the genes studied by RT-qPCR in (**a-b**).

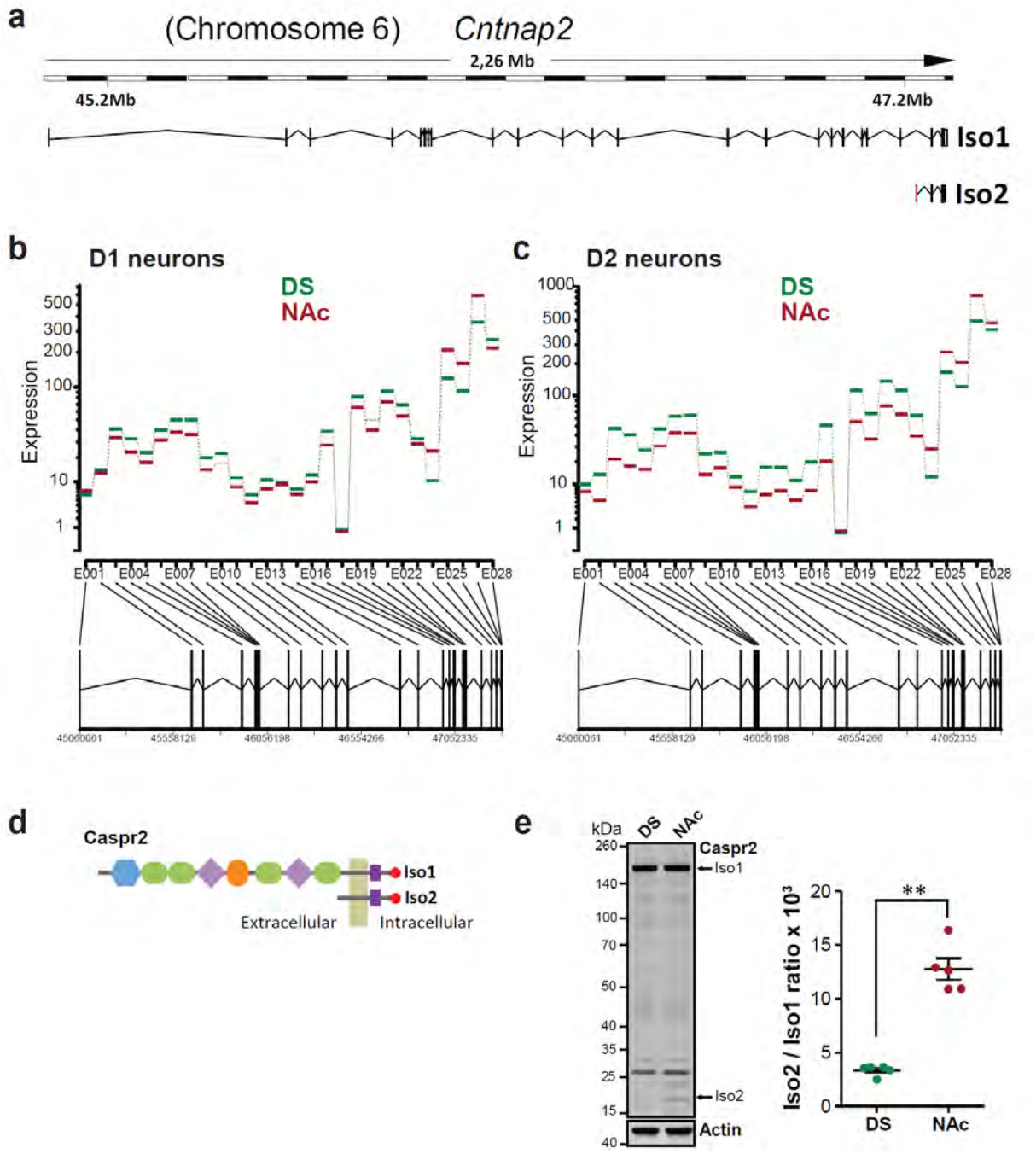

Supplementary Figure 3: Comparison of Cntnap2 exon usage and protein isoform levels in DS and NAc.

a. Structure of the *Cntnap2* gene that codes for the protein Caspr2, which exists as 2 isoforms, Iso1 and Iso2. Iso2 is generated by the use of an internal promoter and exon 24 (in red). **b.** DEX-Seq plot of the relative expression levels of the various exons of *Cntnap2* in DS and NAc of D1-TRAP mice. **c.** DEX-Seq plot of the relative expression levels of the various exons of *Cntnap2* in DS and NAc of D2-TRAP mice. **d.** Schematic representation of the two isoforms of Caspr2 with domain organization indicated ([1]). **e.** Immunoblot analysis of the expression of the two isoforms of Caspr2 in wild-type mouse DS and NAc. **Left panel**, the position of the two quantified isoforms is indicated. **Right panel**, quantification of the protein isoform ratio in samples from 5 mice and normalized to 1 in DS (means ± SEM are indicated). Statistical analyses with two-tailed Mann-Whitney's test, **p < 0.01

a

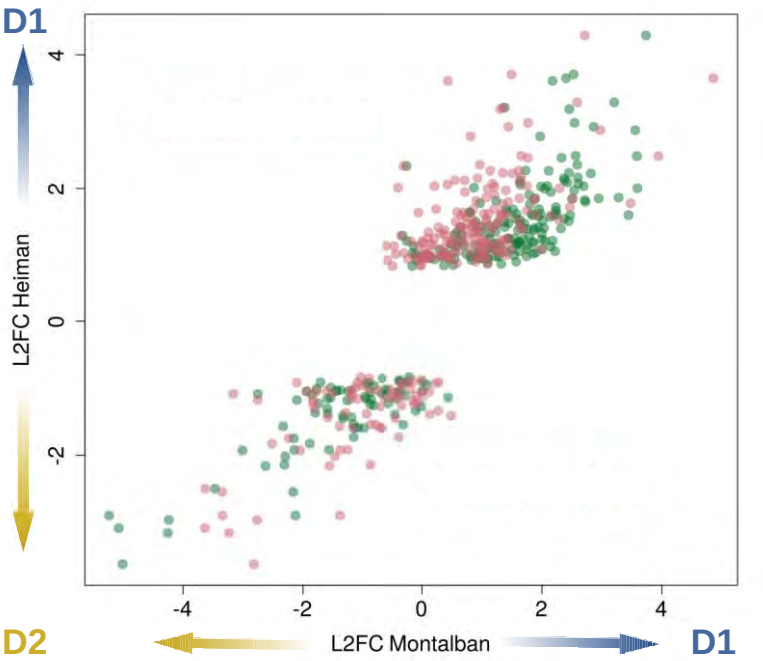
D1
L2FC Heiman
4
2
0
-2
D2
-4
-2
0
2
4
L2FC Montalban
D1

b

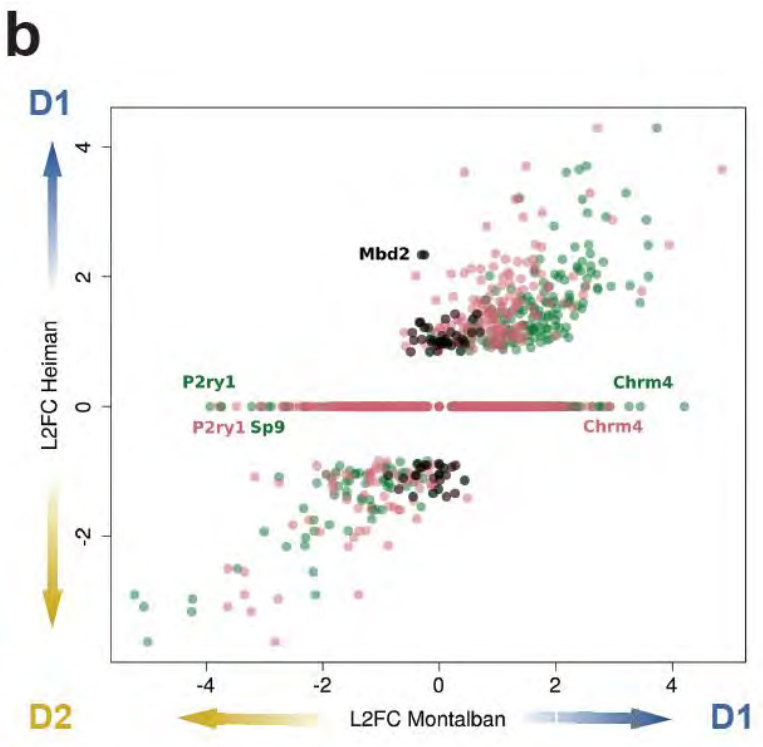
D1
L2FC Heiman
4
2
0
-2
Mbd2
P2ry1
Chrm4
P2ry1 Sp9
Chrm4
D2
-4
-2
0
2
4
L2FC Montalban
D1

c

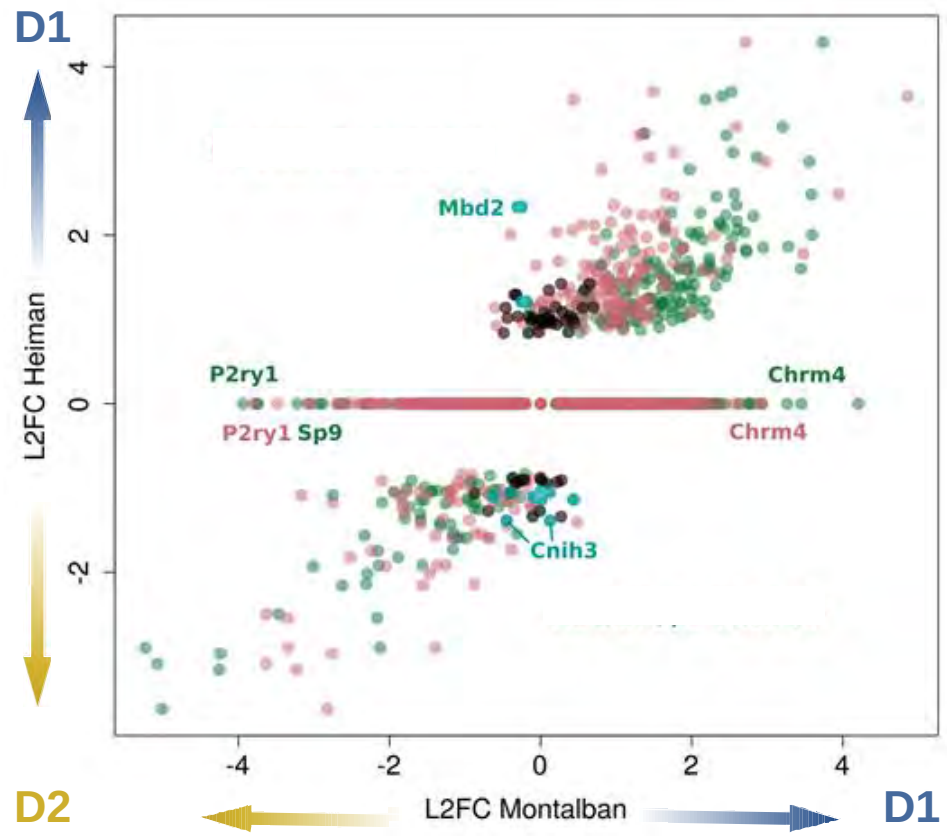
D1
L2FC Heiman
4
2
0
-2
Mbd2
P2ry1
Chrm4
P2ry1 Sp9
Chrm4
Cnih3
-4
-2
0
2
4
D2
L2FC Montalban
D1

d

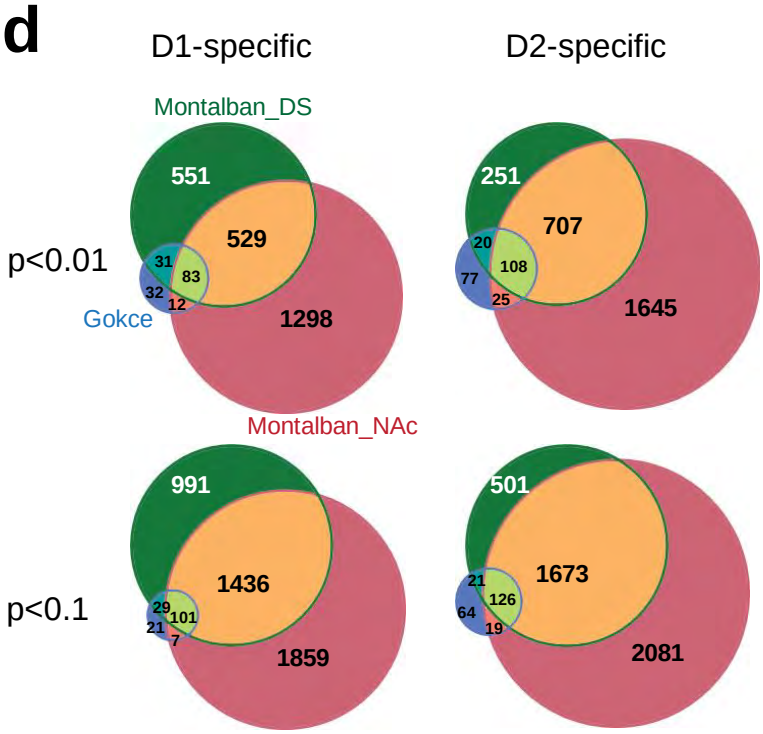
D1-specific
D2-specific
Montalban_DS
p<0.01
551
529
31
83
32
12
Gokce
1298
Montalban_NAc
251
707
20
108
77
25
1645
p<0.1
991
1436
29
101
21
7
1859
501
1673
21
126
64
19
2081

Supplementary Figure 4: Comparison of the results of the current study with previous reports on D1/ D2 neuron differences.

a. mRNAs differentially expressed between D1 and D2 neurons in Heiman et al.[2] (Y axis, log2 fold-changes [L2FC] Heiman) and in the current study (X axis, L2FC Montalban) in the DS (green) or the NAc (magenta). After exclusion of the BAC genes, 248 mRNAs were confirmed in the current study and the correlation between L2FC was very good (DS, R = 0.91, p = 4.9 10^{-94}, NAc, R = 0.83, p = 1.54 10^{-63}). Note that each gene product was plotted twice, against our values in DS and NAc. **b.** Same as in **a** but including also the 33 mRNAs found to be differentially expressed in Heiman et al. but not here (black). With the exception of Mbd2, the L2FC changes observed for those mRNAs are on the lower end of the scale in both studies. The 5042 mRNAs found differentially expressed in our study but not in Heiman et al. are also shown (dots aligned horizontally on L2FC Heiman 0). They include mRNAs whose expression differs by up to one order of magnitude between D1 and D2 neurons (horizontal dispersion of the dots at y = 0; e.g. *P2ry1*, *Sp9* both enriched in D2 neurons and *Chrm4*, enriched in D1 neurons). **c.** Same as in **b** but also indicating 7 mRNAs (blue) identified as different between D1 and D2 by Heiman et al. but neither in our current study nor in Ho et al.[3]. They include *Mdb2* and the cornichon 3 homolog *Cnih3*, which showed the strongest absolute L2FC in Heiman *et* al. Excluding these mRNAs reduces the range of log2 fold changes for our possible false negatives to [-1.34, 1.42]. **d.** Venn diagram comparing the results of our study with those of Gokce *et al*.[4]. Eighty % of their D1-specific mRNAs were also found D1-specific in our study, as were 67% of their D2-specific mRNAs. Most of the genes we did not confirm, exhibited a low expression (e.g. *Rbp4*) and/or a low fold-change (|L2FC|<1), and often an opposite D1 vs D2 specificity (**Supplementary Tables 14a-b**). Increasing the adjusted p-value significance threshold from <0.01 to <0.1 (as in Ref[2]) in our study, recovered only 11 and 13 genes specific for D1 and D2 respectively, found differentially expressed in Refs[2] and[3], but not in another single-cell RNA-Seq analysis[4]. Conversely, using such a less stringent threshold would have increased the number of mRNAs differentially expressed between D1 and D2 neurons to 4878 in the DS and 7302 in the NAc, probably containing a large number of false positive. Most of the genes we did not confirm exhibited a low expression (e.g. *Rbp4*) and/or a low fold-change (|Log_2FC|<1), and often an opposite D1/D2 specificity. Discrepancies may originate from sampling bias or stochastic dropout for the genes with low base counts in single-cells. Overall it is important to underline that single-cell sequencing and TRAP-Seq provide different types of information that are complementary with consistent results in their area of overlap.

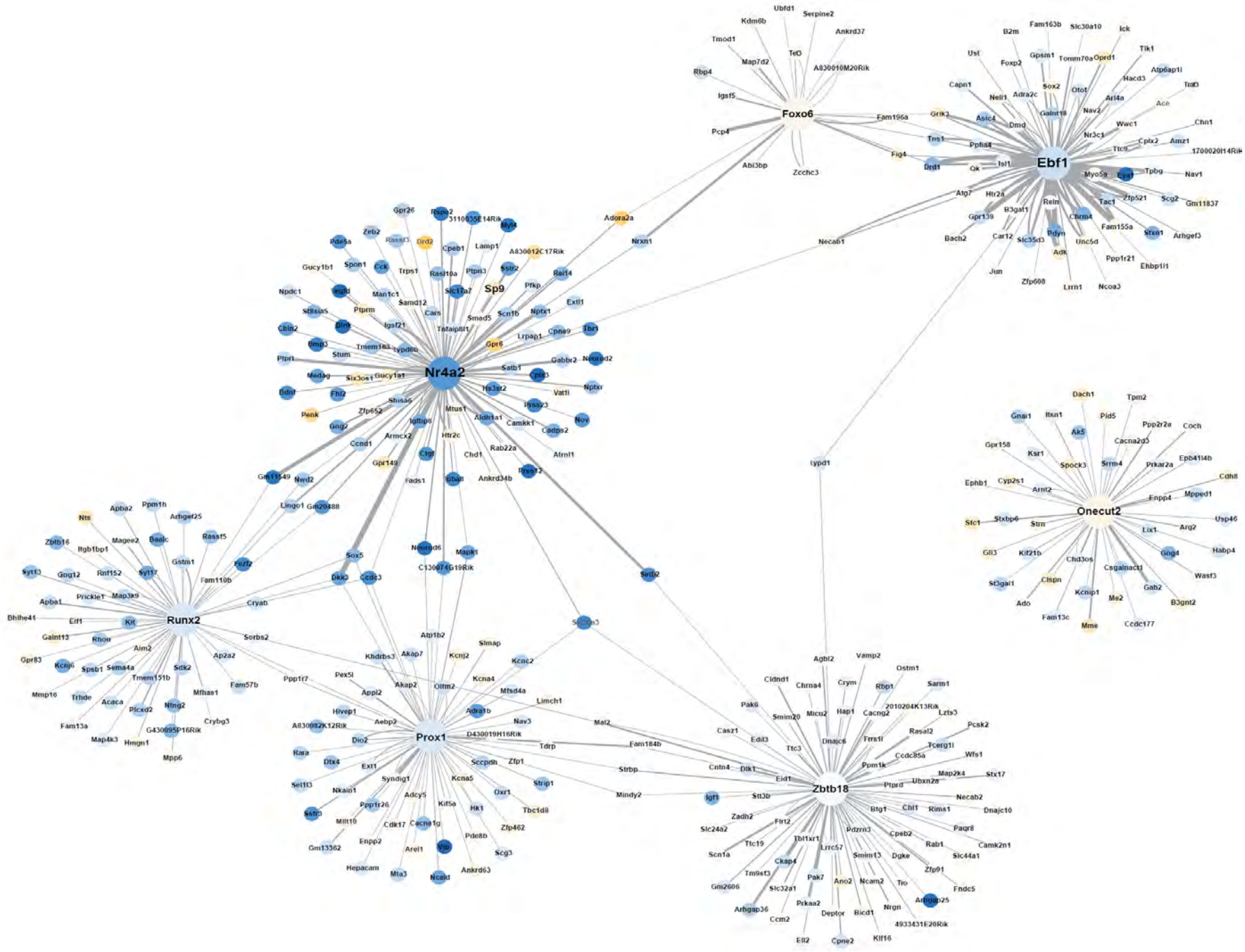
Foxo6
Ebf1
Nr4a2
Runx2
Prox1
Zbtb18
Onecut2
Sp9
Ubfd1
Serpine2
Kdm6b
Ankrd37
Tmod1
Map7d2
TeO
A830010M20Rik
Rbp4
Igsf5
Pcp4
Abi3bp
Zcchc3
Fam196a
Fig4
Tns1
Ppfia4
Drd1
Ok
Isl1
Grik3
Asic4
Dmd
Fam163b
Slc30a10
B2m
Ick
Ust
Foxp2
Gpsm1
Tomm70a
Oprd1
Tik1
Atp6ap1l
Hacd3
Capn1
Nell1
Adra2c
Sox2
Otot
Arl4a
Galnt18
Nav2
Ace
Wwc1
Chn1
Nr3c1
Cplx2
Amz1
Ttc9
1700020I14Rik
Myo5a
Epn1
Tpbg
Nav1
Atg7
Htr2a
B3galt1
Reln
Tac1
Zfp521
Scg2
Gm11837
Gpr139
Chrm4
Fam155a
Strn1
Arhgef3
Bach2
Car12
Slc35d3
Pdyn
Unc5d
Adk
Ppp1r21
Ehbp1l1
Jun
Zfp608
Lrrn1
Ncoa3
Necab1
Adora2a
Nrxn1
Gpr26
Rasa2
3110035E14Rik
Myl4
Zeb2
Rassf3
Drd2
Cpeb1
Lamp1
A830012C17Rik
Pde5a
Gucy1b1
Spon1
Cck
Trps1
Rasl10a
Ptpn3
Sstr2
Rarl4
Pfkp
Npdc1
Neurl1
Man1c1
Samd12
Scl17a7
Cars
Smad5
Scn1b
Nptx1
Extl1
St8sia5
Ptprm
Igsf21
Tnfaip8l1
Cbln2
Blnk
Tbr1
Cpne9
Lrpap1
Gpr6
Bmp3
Tmem163
Dpysl5
Stum
Ptpn1
Gabbr2
Neurod2
Satb1
Cpd
Med30
Six3os1
Gucy1a1
Bdnf
Fhl2
Hs3st2
Vatl1
Nptxr
Shisa6
Penk
Zfp652
Mtus1
Hpse2
Igfbpl1
Aldh1a1
Camkk1
Nov
Gng2
Ccnd1
Armcx2
Htr2c
Codps2
Ctgf
Chd1
Rab22a
Afmid
Gpr149
Gm11549
Nwd2
Fads1
Uba6
Ankrd34b
Prss12
Lingo1
Gm20488
Lypd1
Dach1
Tpm2
Gnai1
Itsn1
Pid5
Ppp2r2a
Coch
Ak5
Cacna2d3
Gpr158
Ksr1
Spock3
Srrm4
Prkar2a
Epb41l4b
Ephb1
Cyp2s1
Arnt2
Cdh8
Enpp4
Mpped1
Stc1
Stxbp6
Strn
Usp46
Lix1
Arg2
Gli3
Klf21b
Chd3os
Gng4
Habp4
Csgalnact1
St3gal1
Clspn
Gab2
Wasf3
Kcnip1
Me2
B3gnt2
Ado
Fam13c
Mme
Ccdc177
Nts
Apba2
Ppm1h
Arhgef25
Zbtb16
Magee2
Baalc
Rassf5
Hgb1bp1
Gstm1
Pcdh7
Syt13
Gng12
Rnf152
Syt17
Fam110b
Sox5
Dkk3
Ccdc3
Neurod6
Mapk1
C130074G19Rik
Satb2
Apba1
Prickle1
Map3k9
Cryab
Bhlhe41
Eif1
Kit
Runx2
Galnt13
Rhou
Sorbs2
Gpr83
Aim2
Ap2a2
Kcnj6
Spsb1
Sema4a
Sdk2
Tmem151b
Fam57b
Mmp16
Trhde
Mfhas1
Acaca
Plcxd2
Ntng2
Crybg3
Fam13a
Map4k3
Hmgn1
G430095P16Rik
Mpp6
Atp1b2
Slmap
Khdrbs3
Akap7
Kcnj2
Kcnc2
Ppp1r7
Pex5l
Appl2
Akap2
Olfm2
Kcna4
Mfsd4a
Limch1
Hivep1
Adra1b
Nav3
A830082K12Rik
Aebp2
Dio2
Prox1
D430019H16Rik
Mal2
Rara
Tdrp
Fam184b
Dtx4
Ext1
Sccpdh
Zfp1
Strbp
Syndig1
Kcna5
Strip1
Sel1l3
Nkain1
Adcy5
Oxr1
Mindy2
Ppp1r26
Klf5a
Hk1
Tbc1d8
Satb1
Cdk17
Cacna1g
Zfp462
Mllt10
Pde8b
Gm13362
Enpp2
Arel1
Vsig
Scg3
Hepacam
Mta3
Ncald
Ankrd63
Agbl2
Vamp2
Ostm1
Cldnd1
Chrna4
Crym
Rbp1
Sarm1
Pak6
Micu2
Hap1
Cacng2
2010204K13Rik
Lzts3
Smim20
Casz1
Edil3
Dnajc6
Ttc3
Frrs1l
Rasal2
Pcsk2
Tcerg1l
Ccdc85a
Wfs1
Ppm1k
Cntn4
Dlk1
Eid1
Map2k4
Stx17
Ubxn2a
Ptprd
Igf1
Stt3b
Zbtb18
Necab2
Btg1
Chl1
Rims1
Dnajc10
Zadh2
Flrt2
Slc24a2
Pdzrn3
Paqr8
Cpeb2
Tbl1xr1
Camk2n1
Ttc19
Lrrc57
Rab1
Scn1a
Smim13
Dgke
Slc44a1
Ckap4
Zfp91
Tm9sf3
Pak7
Ano2
Ncam2
Tro
Fndc5
Gm2606
Slc32a1
Arhgap36
Prkaa2
Deptor
Bicd1
Nrgn
Arhgap25
Ccm2
4933431E20Rik
Ell2
Cpne2
Klf16

Supplementary Figure 5: Striatal gene network of transcription factors illustrating connections with mRNAs differentially expressed in D1 and D2 cells.

To evaluate the potential functional importance of TFs in the regulation of transcriptional profiles in adult striatal neurons, we used a gene expression-based network inference procedure and combined the results of CLR[5], a mutual-information-based approach providing undirected edges, and GENIE3[6], a tree-based regression approach providing directed edges, using filtered CPM (see **Supplementary Methods**). We pruned the network by retaining only the edges that connected either one or two of the TFs differentially expressed between DS and NAc. Subnetworks were extracted using gene lists as seeds, retaining only the first neighbors with scores above a threshold. Seven TFs passed the filter and six of them formed a connected subnetwork of clusters. Visualization and analysis of the resulting networks was done using Cytoscape[7], only keeping the 1% edges with the highest scores. The edges that connected either one or two of the TFs differentially expressed between DS and NAc, focusing on TFs specific of D1 cells, are shown. Seven TFs passed the filter and six of them formed a connected subnetwork of clusters (i.e. sharing first neighbors). Nodes are colored according to their relative expression in D1 (blue) and D2 (yellow) neurons. *Nr4a2* and *Ebf1* are surrounded by genes differentially expressed in D1 and D2 cells. The color intensities reflect differential expression and line thickness the reliability of prediction. *Nr4a2* codes for Nurr1, a key TF in the maintenance of dopaminergic neurons, and, in the striatum, is associated with the development of dyskinesia[8,9]. *Ebf1* is known for its role in D1-SPN differentiation[10,11]. These results support the role of *Nr4a2* and *Ebf1* in regulating differences between D1 and D2 SPNs in adult mice.

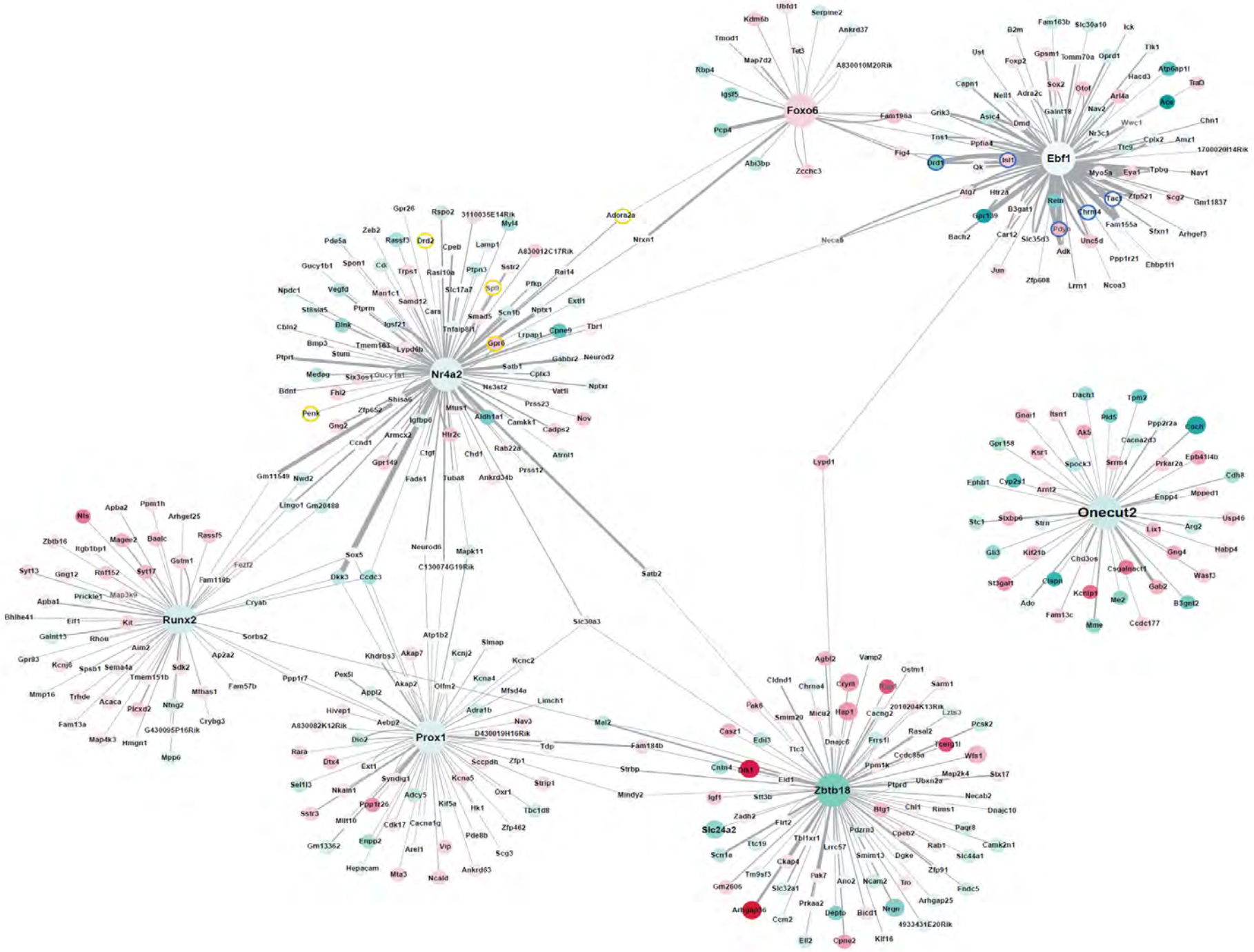
Foxo6
Ebf1
Nr4a2
Runx2
Prox1
Zbtb18
Onecut2
Ubfd1
Kdm6b
Serpine2
Ankrd37
Tmod1
Tet3
Map7d2
A830010M20Rik
Rbp4
Igsf5
Pcp4
Abi3bp
Zcchc3
Fam163b
Slc30a10
Ick
B2m
Ust
Foxp2
Gpsm1
Tomm70a
Oprd1
Tlk1
Atp6ap1l
Hacd3
Capn1
Nell1
Adra2c
Sox2
Otof
Arl4a
Ace
Galnt18
Nav2
Nr3c1
Wwc1
Chn1
Fig4
Ppfia4
Tns1
Grik3
Asic4
Dmd
Cplx2
Amz1
Ttc9
1700020I14Rik
Drd1
Isl1
Qk
Myo5a
Eya1
Tpbg
Nav1
Atg7
Htr2a
Rem
Tac1
Zfp521
Scg2
Gm11837
B3gat1
Chrm4
Fam155a
Sfxn1
Arhgef3
Bach2
Car12
Slc35d3
Unc5d
Adk
Ppp1r21
Ehbp1l1
Jun
Zfp608
Lrrn1
Ncoa3
Necab
Adora2a
Nrxn1
Gpr26
Rspo2
3110035E14Rik
Myl4
Zeb2
Pde5a
Rassf3
Drd2
Cpeb
Lamp1
A830012C17Rik
Gucy1b1
Spon1
Cx
Trps1
Rasl10a
Ptpn3
Sstr2
Rai14
Npdc1
Vegfd
Man1c1
Slc17a7
Spp1
Pfkp
St8sia5
Ptprm
Samd12
Cars
Smad5
Scn1b
Nptx1
Extl1
Cbln2
Blnk
Igsf21
Tnfaip8l1
Cpne9
Tbr1
Bmp3
Tmem163
Lypd6b
Gpr6
Lrpap1
Ptprt
Stum
Gabbr2
Neurod2
Medag
Six3os1
Gucy1a1
Satb1
Cplx3
Bdnf
Fhl2
Hs3st2
Vat1l
Nptxr
Penk
Zfp652
Shisa6
Mtus1
Prss23
Gng2
Igfbp6
Aldh1a1
Camkk1
Nov
Armcx2
Htr2c
Cadps2
Ccnd1
Ctgf
Chd1
Rab22a
Atrnl1
Gpr149
Fads1
Tuba8
Ankrd34b
Prss12
Gm11549
Nwd2
Lingo1
Gm20488
Lypd1
Dach1
Tpm2
Gnai1
Itsn1
Pld5
Ppp2r2a
Coch
Ak5
Cacna2d3
Gpr158
Ksr1
Spock3
Srrm4
Prkar2a
Epb41l4b
Ephb1
Cyp2s1
Amt2
Cdh8
Enpp4
Mpped1
Stc1
Stxbp6
Strn
Usp46
Lix1
Arg2
Gli3
Klf21b
Chd3os
Gng4
Habp4
Csgalnact1
Wasf3
St3gat1
Ckap4
Gab2
Ado
Kctd1
Me2
B3galt2
Fam13c
Mme
Ccdc177
Nfs
Apba2
Ppm1h
Arhgef25
Zbtb16
Itgb1bp1
Magee2
Baalc
Rassf5
Gstm1
Syt13
Gng12
Rnf152
Syt17
Fam110b
Fezf2
Apba1
Prickle1
Map3k9
Cryab
Bhlhe41
Eif1
Kit
Galnt13
Rhou
Sorbs2
Gpr83
Kcnj6
Spsb1
Sema4a
Aim2
Sdk2
Ap2a2
Tmem151b
Mmp16
Trhde
Acaca
Mthas1
Fam57b
Plcxd2
Ntng2
Crybg3
Fam13a
G430095P16Rik
Map4k3
Hmgn1
Mpp6
Sox5
Dkk3
Ccdc3
Fezf2
Neurod6
Mapk11
C130074G19Rik
Satb2
Slc30a3
Atp1b2
Slmap
Khdrbs3
Akap7
Kcnj2
Kcnc2
Pex5l
Akap2
Olfm2
Kcna4
Ppp1r7
Appl2
Mfsd4a
Limch1
Adra1b
Hivep1
Aebp2
A830082K12Rik
Nav3
Mal2
Dio2
D430019H16Rik
Fam184b
Rara
Tdp
Dtx4
Ext1
Sccpdh
Zfp1
Strbp
Sel1l3
Syndig1
Kcna5
Strip1
Nkain1
Adcy5
Oxr1
Mindy2
Sstr3
Ppp1r26
Kif5a
Hk1
Tbc1d8
Mllt10
Cdk17
Cacna1g
Zfp462
Gm13362
Enpp2
Arel1
Vip
Pde8b
Scg3
Hepacam
Mta3
Ncald
Ankrd63
Agbl2
Vamp2
Ostm1
Cldnd1
Chrna4
Crym
Sarm1
Pak6
Smim20
Micu2
Hap1
Cacng2
2010204K13Rik
Lzts3
Pcsk2
Casz1
Edil3
Dnajc6
Frrs1l
Rasal2
Ttc3
Ccdc85a
Tceng1l
Wfs1
Ppm1k
Map2k4
Stx17
Cntn4
Dlk1
Eid1
Ptprd
Ubxn2a
Necab2
Igf1
Stt3b
Btg1
Chl1
Rims1
Dnajc10
Zadh2
Slc24a2
Flrt2
Pdzrn3
Cpeb2
Paqr8
Tbl1xr1
Ttc19
Lrrc57
Rab1
Camk2n1
Scn1a
Ckap4
Smim13
Dgke
Slc44a1
Tm9sf3
Pak7
Ano2
Ncam2
Tro
Zfp91
Gm2606
Slc32a1
Fndc5
Prkaa2
Arhgap25
Arhgap36
Depto
Bicd1
Nrgn
Ccm2
4933431E20Rik
Eif2
Cpne2
Klf16

Supplementary Fig. 6: Striatal gene network of transcription factors illustrating connections with genes differentially expressed in DS and NAc.

Same network as in **Supplementary Figure 5**, except that nodes are colored according to their relative expression in DS (green) and NAc (red). Genes linked to *Onecut2* and *Zbtb18* are strongly differentially expressed in DS and NAc. The color intensities reflect differential expression and line thickness the reliability of prediction. *Onecut2* is a homeobox gene associated with neuronal differentiation[12] whose first neighbors include genes enriched in DS (e.g., *Coch, Tpm2, Dach1, Clspn, B3gnt2, Cyp2s1, Pld5, Me2*). *Zbtb18* mRNA encodes a transcriptional repressor of key proneurogenic genes whose mutation is implicated in intellectual deficit[13]. *Zbtb18*'s first neighbors include genes enriched in NAc (e.g., *Arhgap36, Wfs1, Crym*, *Dlk1, Tcerg1l, Hap1*) or in DS (e.g., *Nrgn, Slc24a2*; see **Supplementary Tables 6a**,**b**). The genes connected to *Nr4a2* and *Ebf1*, and typical of D1 or D2 cells (see **Supplementary Figure 5**) are indicated by a blue or yellow lining respectively.

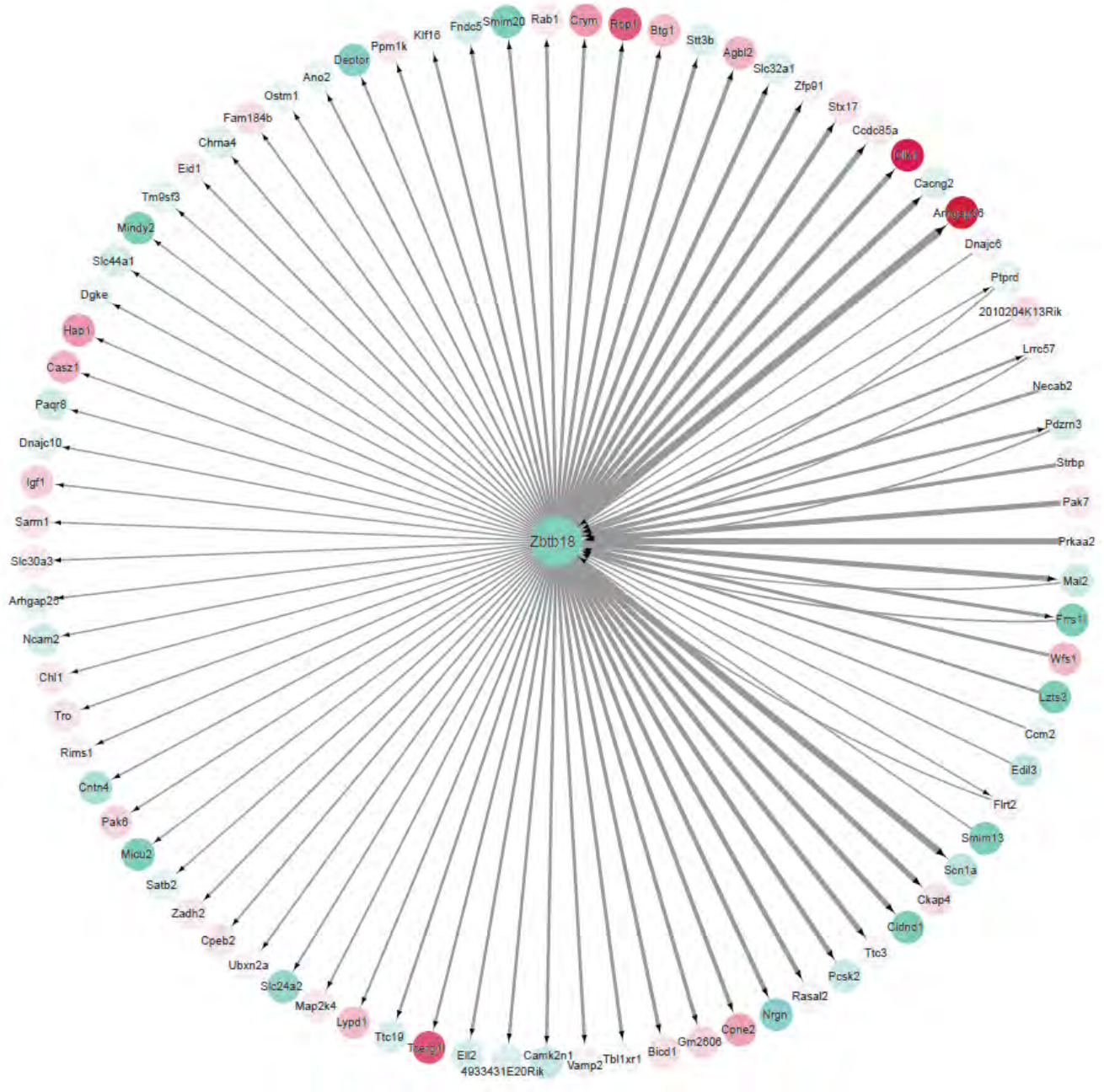

Supplementary Figure 7: Gene expression-based network inference of Zbtb18 regulations in SPNs. Only influences passing our threshold are shown. Arrows indicate the direction of the influences. Line thickness reflects the reliability of prediction. Gene nodes are colored according to their relative expression in DS (green) or NAc (red). Among threshold-passing influences, 66 are coming solely from *Zbtb18*, 10 are solely going to *Zbtb18* and 7 are bidirectional, but with a higher weight of outgoing interaction.

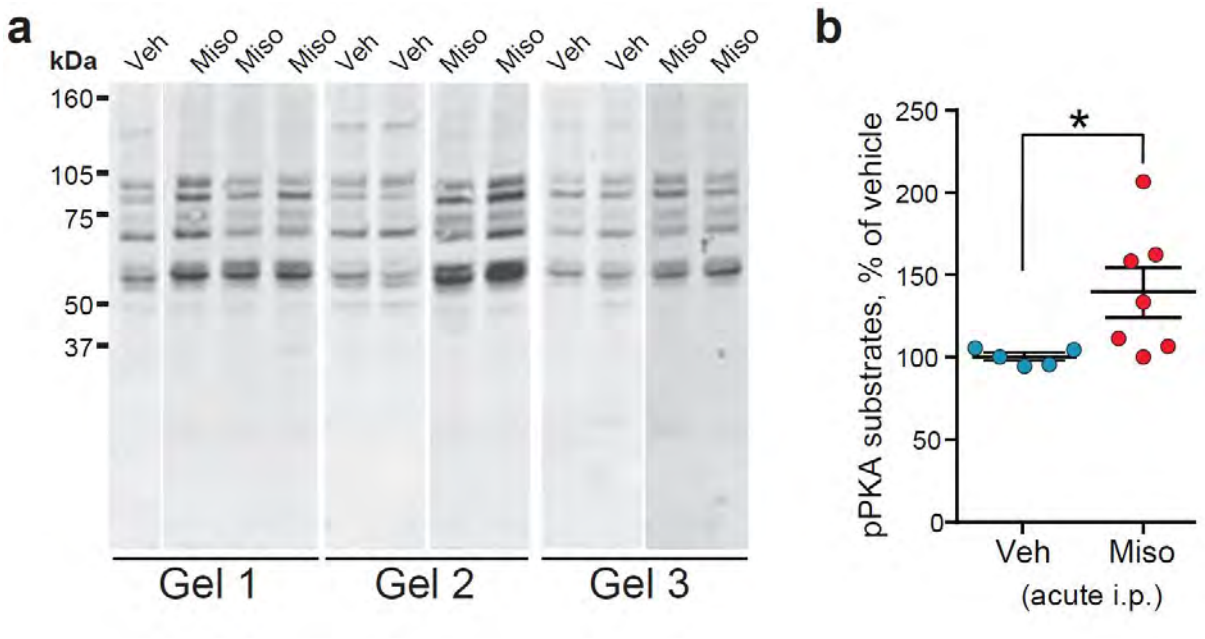

Supplementary Fig. 8: Misoprostol increases phosphorylation of PKA-substrates in the dorsal striatum.

a. To test whether the effects of stimulating PGE2 receptors were detected in the DS. Misoprostol, a PGE2 agonist (**Miso**, 0.1 mg.kg^{-1}, 7 mice) or vehicle (**Veh**, 5 mice) was injected i.p. Mice were sacrificed 30 min later, striatal extracts were analyzed by immunoblotting with a phosphoPKA-substrate antibody (three different gels were run, as indicated). The positions of molecular weight markers are indicated in **kDa**. **b.** Immunoreactivity was quantified by densitometry measurement of the whole lane and expressed as percent of the mean in vehicle-treated mice (**right panel**). Statistical analyses with two-tailed Mann-Whitney's test (see **Supplementary Table 19**). * $p < 0.05$.

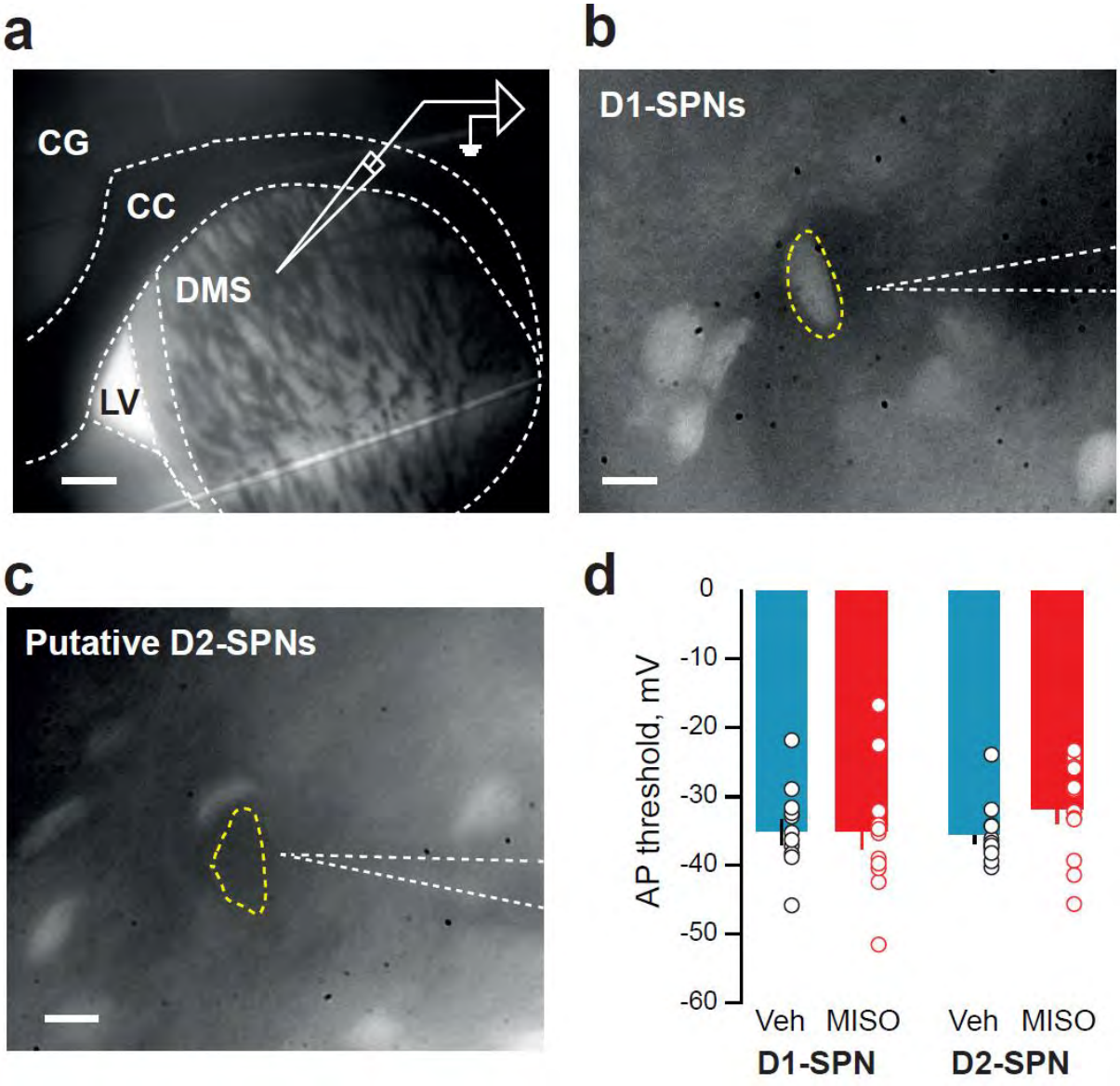

Supplementary Fig. 9: Study of misoprostol effects on electrophysiological properties of DS D1- and D2-SPNs.

a. Male D1R-Cre x Ai14 tdTomato reporter mice were injected i.p. with vehicle or misoprostol (0.1 mg/kg). Thirty minutes later mice were sacrificed and brain slices were made for patch clamp electrophysiological experiments. D1- and putative D2-SPNs in the dorsomedial striatum (DMS) were identified based on red fluorescence and morphology and patched. CG, cingulate cortex, CC, corpus callosum, LV, lateral ventricle. **b.** Identification of a red fluorescent D1-SPN (yellow dashed lane). **c.** Identification of a non-fluorescent SPN identified as a putative D2-SPN. **d.** In patch-clamp experiment as in Fig. 4, the action potential threshold was not affected by misoprostol in either cell type (two-way ANOVA, $F < 1$ for all factors).

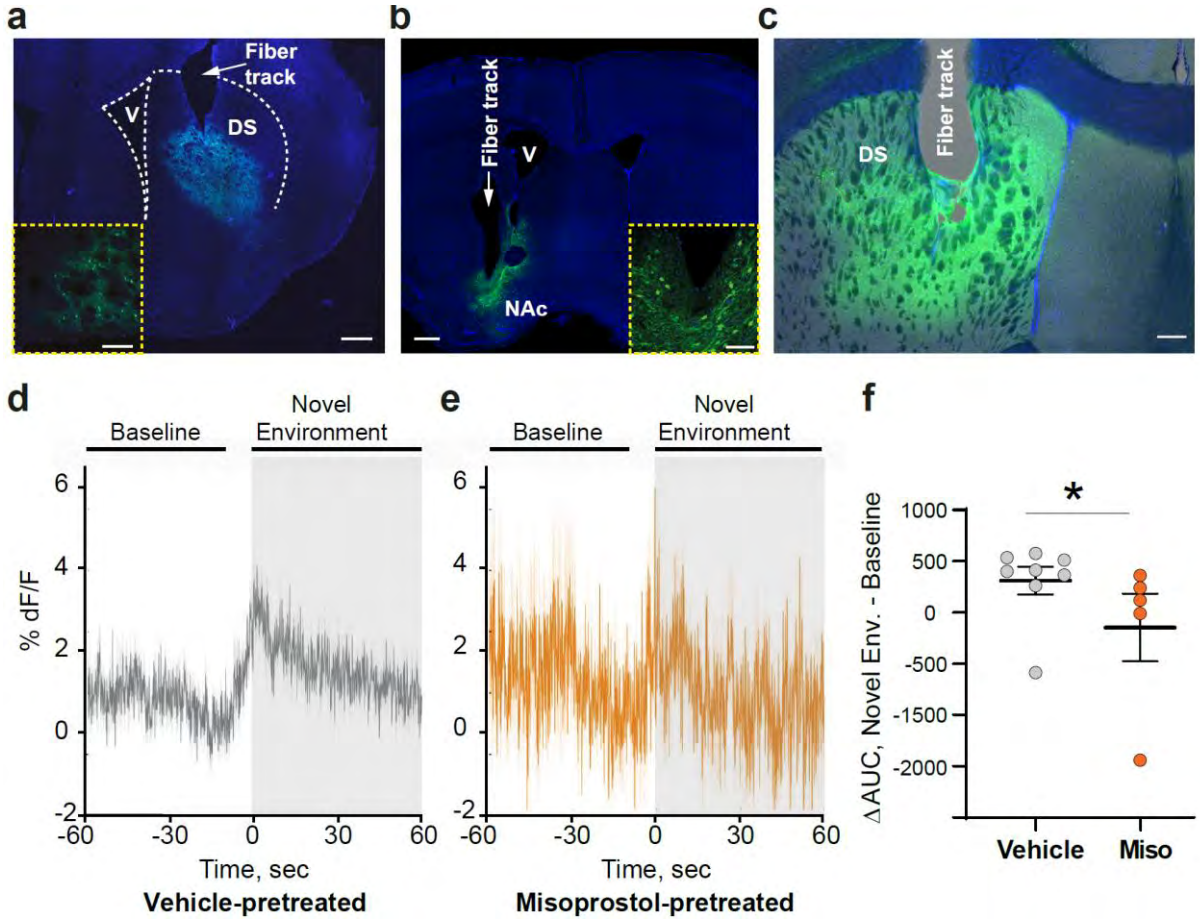

Supplementary Fig. 10: Fiber photometry recording of striatal neurons Ca^{2+} activity and effects of misoprostol on NAc D2-neurons.

a-c. Representative histological controls for fiber implantation and GCaMP6f expression. Mosaic of confocal images in representative mice used for fiber photometry DAPI (blue)/ GCaMP6f (green). Mice were stereotactically injected with pAAV.Syn.Flex.GCaMP6f.WPRE.SV40 in the region of interest and the recording cannula implanted 100 µm above. (**a**, **b**) The fiber was placed in the DS (**a**) or the NAc (**b**) of a *Drd2*-Cre mouse, scale bar, 200 µm. Inset: higher magnification of a different section, scale bar 150 µm. (**c**) The fiber was placed in the DS of a *Drd1*-Cre mouse, scale bar 400 µm. **d-f.** Misoprostol pretreatment decreases D2 neurons activity in the NAc during exploration of a novel environment (mouse placed in a new cage). Activity was evaluated by fiber photometry in the NAc of *Drd2*-Cre mice stereotactically injected with an AAV GCaMP6f (as in **b**). Each mouse was recorded twice with an interval ≥ 1 day, 30 min after receiving either vehicle or misoprostol (**Miso**, 0.1 $mg.kg^{-1}$, i.p.) in random order. **d.** Average traces of mice injected with vehicle and placed for 1 min in a novel environment, as indicated. **e**. Same as in (**d**) for mice injected with misoprostol. **f.** Plot of area under the curve (AUC) in **d** and **e** during the novel environment exploration (60 s) minus the AUC during baseline (50 s) in mice treated with vehicle (n = 8) or misoprostol (n = 5). Statistical analysis two-tailed Mann-Whitney test, p = 0.03.

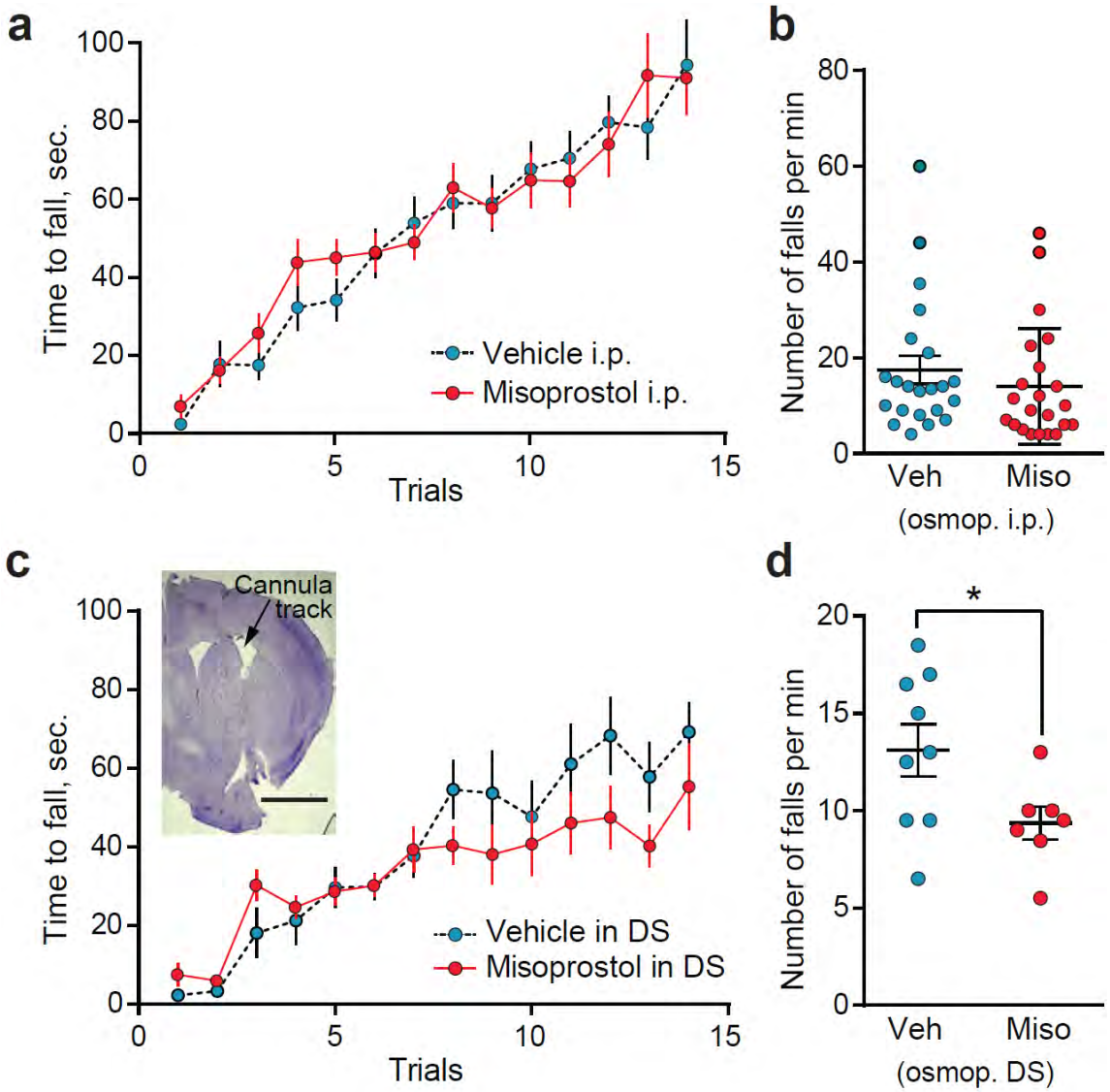

Supplementary Fig. 11: Rotarod learning in mice receiving chronic misoprostol infusion intraperitoneally or in the DS.

a. Wild-type mice were implanted on day 1 with an i.p. osmotic minipump containing either vehicle (Veh) or misoprostol (Miso, 50 µg kg^{-1} day^{-1}). They were tested on an accelerating rotarod starting at day 9 (4 trials per day). Latency to fall during the learning phase was recorded. Two-way repeated measures ANOVA showed an effect of time ($F_{(11, 562)} = 23.36$, $p < 10^{-4}$), but not of treatment ($F_{(11,562)} = 0.05$, $p = 0.81$), n = 14 mice per group. **b.** The same mice as in (**a**) were tested 24 h after the last training session at a fixed speed of 24 r.p.m. After each fall the mouse was placed back on the rod and the number of falls counted until the time spent on the rod reached 1 min. Two-tailed Mann-Whitney test, $p = 0.17$. **c.** Wild-type mice were implanted on day 1 with two subcutaneous osmotic minipumps containing Veh or Miso and linked to a catheter connected to a cannula implanted in each DS and trained on an accelerating rotarod as in **a**. Two-way repeated measures ANOVA showed an effect of time ($F_{(13, 221)} = 28.68$, $p < 10^{-4}$), but not of treatment ($F_{(1,221)} = 0.64$, $p = 0.43$), n = 9-10 mice per group. **Inset:** Nissl-stained coronal brain section showing a cannula track (**arrow**) in the DS. Scale bar, 2 mm. **d.** The same mice as in (**c**) were tested 24 h after the last training session at a fixed speed of 24 r.p.m. Two-tailed Student's t test, $t_{14} = 2.2$, $p = 0.04$. See detailed statistical analyses in **Supplementary Table 19.**

References for Supplementary Figures

1. Saint-Martin M, Joubert B, Pellier-Monnin V, Pascual O, Noraz N, Honnorat J. Contactin-associated protein-like 2, a protein of the neurexin family involved in several human diseases. *Eur J Neurosci* 2018; **48**(3)**:** 1906-1923.

2. Heiman M, Schaefer A, Gong S, Peterson JD, Day M, Ramsey KE *et al.* A translational profiling approach for the molecular characterization of CNS cell types. *Cell* 2008; **135**(4)**:** 738-748.

3. Ho H, Both M, Siniard A, Sharma S, Notwell JH, Wallace M *et al.* A Guide to Single-Cell Transcriptomics in Adult Rodent Brain: The Medium Spiny Neuron Transcriptome Revisited. *Front Cell Neurosci* 2018; **12:** 159.

4. Gokce O, Stanley GM, Treutlein B, Neff NF, Camp JG, Malenka RC *et al.* Cellular Taxonomy of the Mouse Striatum as Revealed by Single-Cell RNA-Seq. *Cell Rep* 2016; **16**(4)**:** 1126-1137.

5. Faith JJ, Hayete B, Thaden JT, Mogno I, Wierzbowski J, Cottarel G *et al.* Large-scale mapping and validation of Escherichia coli transcriptional regulation from a compendium of expression profiles. *PLoS biology* 2007; **5**(1)**:** e8.

6. Huynh-Thu VA, Irrthum A, Wehenkel L, P. G. Inferring regulatory networks from expression data using tree-based methods. *PLoS One* 2010; **5**(9)**:** e12776.

7. Shannon P, Markiel A, Ozier O, Baliga NS, Wang JT, Rmage D *et al.* Cytoscape: A Software Environment for Integrated Models of Biomolecular Interaction Networks. *Genome Res* 2003; **13:** 2498-2504.

8. Sellnow RC, Steece-Collier K, Altwal F, Sandoval IM, Kordower JH, Collier TJ *et al.* Striatal Nurr1 Facilitates the Dyskinetic State and Exacerbates Levodopa-Induced Dyskinesia in a Rat Model of Parkinson's Disease. *J Neurosci* 2020; **40**(18)**:** 3675-3691.

9. Steece-Collier K, Collier TJ, Lipton JW, Stancati JA, Winn ME, Cole-Strauss A *et al.* Striatal Nurr1, but not FosB expression links a levodopa-induced dyskinesia phenotype to genotype in Fisher 344 vs. Lewis hemiparkinsonian rats. *Exp Neurol* 2020; **330:** 113327.

10. Garel S, Marin F, Grosschedl R, Charnay P. Ebf1 controls early cell differentiation in the embryonic striatum. *Development* 1999; **126**(23)**:** 5285-5294.

11. Lobo MK, Yeh C, Yang XW. Pivotal role of early B-cell factor 1 in development of striatonigral medium spiny neurons in the matrix compartment. *J Neurosci Res* 2008; **86**(10)**:** 2134-2146.

12. van der Raadt J, van Gestel SHC, Nadif Kasri N, Albers CA. ONECUT transcription factors induce neuronal characteristics and remodel chromatin accessibility. *Nucleic Acids Res* 2019; **47**(11)**:** 5587-5602.

13. de Munnik SA, Garcia-Minaur S, Hoischen A, van Bon BW, Boycott KM, Schoots J *et al.* A de novo non-sense mutation in ZBTB18 in a patient with features of the 1q43q44 microdeletion syndrome. *Eur J Hum Genet* 2014; **22**(6)**:** 844-846.